第 31 卷第 3 期 无 机 化 学 学 报 Vol.31 No.3
2015 年 3 月 CHINESE JOURNAL OF INORGANIC CHEMISTRY 555-564

由羧酸和含氮杂环配体构筑从核到双链结构的金属有机骨架

顾晓敏[1] 王 蕾[1] 单月霞[1] 张文莉*,[1] 陈 钦[1] 倪 良[1] 姚 加[2]
([1]江苏大学化学化工学院,镇江 212013)
([2]浙江大学化学系,杭州 310027)

摘要：通过水热法合成了 3 个配合物{[Mn(4,4′-oba)(Medpq)]Medpq}$_n$ (**1**),[Mn$_2$(4,4′-oba)$_2$(MOPIP)$_4$]·2H$_2$O (**2**)和[Cd(ox)(MOPIP)$_2$]·2H$_2$O (**3**)(4,4′-H$_2$oba=4,4′-二苯醚二甲酸,H$_2$ox=草酸,Medpq=2-甲基吡嗪[3,2-*f*:2,3′-*h*]喹喔啉,MOPIP=2-(-甲氧基)-氢-咪唑[4,5-*f*][1,10]菲咯啉),并通过 X-射线单晶衍射分析得出它们的晶体结构。配合物 1 表现为一个一维的双链结构。 配合物 2 和 3 分别为双核和单核的零维离散结构,在 π-π 堆积和氢键的作用下,进一步形成了三维网络状结构。结构分析结果表明氮杂环和二羧酸配体对配合物的结构有很大影响。此外,在室温下对配合物 **2** 和 **3** 进行了荧光性质分析。

关键词：荧光性质；结构多样性；相互作用；自然键轨道分析
中图分类号：O614.7+11；O614.24+2 **文献标识码**：A **文章编号**：1001-4861(2015)03-0555-10
DOI：10.11862/CJIC.2015.091

Frameworks of Metal Dicarboxylate Complexes: from Nuclear Structures to Double Chains Based on N-containing Ligands

GU Xiao-Min[1] WANG Lei[1] SHAN Yue-Xia[1] ZHANG Wen-Li*,[1] CHEN Qin[1] NI Liang[1] YAO Jia[2]
([1]*School of Chemistry and Chemical Engineering, Jiangsu University, Zhenjiang, Jiangsu* 212013, *China*)
([2]*Department of Chemistry, Zhejiang University, Hangzhou* 310027, *China*)

Abstract: Three complexes have been obtained by the reaction of metal (Mn(Ⅱ), Cd(Ⅱ)), 5,6-substituted 1,10-phen derivatives with two carboxylic acids, 4,4′-oxybis (benzoic acid)(4,4′-H$_2$oba) and oxalic acid (H$_2$ox). The crystal structures of the resulting complexes , namely {[Mn(4,4′-oba)(Medpq)]Medpq}$_n$ (**1**), [Mn$_2$(4,4′-oba)$_2$(MOPIP)$_4$]·2H$_2$O (**2**), and [Cd(ox)(MOPIP)$_2$]·2H$_2$O (**3**) (Medpq=2-methyldipyrido-[3,2-*f*:2,3′-h]quinoxaline, MOPIP=2-(4-methoxyphenyl)-1*H*-imidazo[4,5-*f*][1,10]phenanthroline]), have been elucidated using their single-crystal X-ray diffraction analysis. Diverse structures are observed for these complexes. Compound **1** contains double chains, which are further stacked via hydrogen bonding interactions to form layers. Compound **2** features dinuclear structures, which are connected by strong $\pi\cdots\pi$ and hydrogen bonding interactions to result in layer structures. Compound **3** contains mononuclear structures and extended to chain and layer structures by $\pi\cdots\pi$ and hydrogen bonding interactions. The differences among these structures indicate that the size of the rigid chelating ligands and the flexibility of carboxylate have important effects on the structures of their complexes. The fluorescent properties of **2** and **3** were studied in the solid state at room temperature. CCDC: 1021348, **1**; CCDC: 1021349, **2**; CCDC: 1021347, **3**.

Key words: fluorescent property; structural diversity; interactions; NBO analysis

收稿日期:2014-09-01。收修改稿日期:2015-01-06。
江苏大学高级人才启动基金项目(No.14JDG053),江苏省博士后科学基金(No.1401176C)资助项目。
*通讯联系人。E-mail:zhangwl@ujs.edu.cn

Current interest in coordination polymers is rapidly expanding due to their intriguing architectures[1-2] and potential applications in the areas of catalysis, separation analysis, gas adsorption, sensors, and in electronic and magnetic devices[3-5]. But it is still a great challenge to predict the structures and properties of metal-organic coordination polymers[6-7]. The final structures of metal-organic coordination polymers are dependent upon multiple factors[8-9], among which the most important ones are the geometrical and electronic properties of the metal ions and ligands. The structural geometry can be controlled and modulated by selecting the coordination geometry of metal ions and the chemical nature of the terminal and bridging ligands. The common process to control the structures of the coordination polymers is using N-heterocyclic ligands and polycarboxylate[10-11]. The 5,6-substituted 1,10-phen derivatives as chelating terminal ligands have two N-donors, which can play many kinds of roles in coordination polymers[12-16]. Especially, the conjugate aromatic nucleus will contribute to form interesting structures through aromatic $\pi \cdots \pi$ stacking and hydrogen bonding interactions. 4,4′ -oxybis (benzoic acid)(H_2oba) is a flexible carboxylate ligand, where the two phenyl rings can freely twist around the -O- group to meet the requirements of the coordination geometries of metal ions in the assembly process. So, The long 4,4′ -oba ligand is a very good bridging ligand[17-20].

In this context, metal (Mn, Cd) ions with d^{10} configuration are particularly promising due to their wider range of coordination numbers together with their applications[21-23] in luminescence and biological activities. Considering these aspects, it was found interesting to synthesize complexes of Mn(Ⅱ) and Cd(Ⅱ) based on 5,6-substituted 1,10-phen derivatives with two different types of ligand frameworks (4,4′-H_2oba and H_2ox) without use of a third component as spacer.

1 Experimental section

1.1 Materials and methods

The chelating ligands MOPIP and Medpq were synthesized according to the previous literature method[24]. Other reagents and solvents for synthesis were purchased from commercial sources and used as received. Transmission mode FT-IR spectra were obtained as KBr pellets between 400 and 4 000 cm^{-1} using a Nicolet Nexus 470 infrared spectrometer. Elemental analysis was carried out with a Perkin-Elmer 240C analyzer. Thermogravimetric analysis (TG) was performed on a Germany Netzsch STA449C at a heating rate of 10 ℃·min^{-1} in nitrogen. Powder X-ray diffraction patterns were obtained using a pinhole camera (Shimadzu) operating with a point focused Cu radiation in the 2θ range from 5° to 50° with a scan rate of 0.2°·s^{-1}. Fluorescence measurement was carried out at room temperature with a Cary Eclipse spectrometer.

1.2 Computational procedures

All computations were performed using Gaussian 03 program package[25] for complex **1** and **3**. The molecular structures for the calculation were all from the initial X-ray structures of the complexes, which were used for the geometry optimization. All the subsequent calculations were performed based on the optimized geometries. Natural bond orbital (NBO) analyses were performed by applying 6-31+G(d) basis set for C, H, O, N atoms, and the effective core potential basis set Lanl2dz for metal atoms.

1.3 Synthesis of the complexes 1~3

{[Mn(4,4′-oba)(Medpq)]Medpq}$_n$ (**1**): A mixture of $MnCl_2 \cdot 4H_2O$ (0.099 g, 0.5 mmol), 4,4′-H_2oba (0.121 g, 0.5 mmol), Medpq (0.124 g, 0.5 mmol), Et_3N (0.101 g, 1 mmol) and H_2O (18 mL) was placed in a 25 mL Teflon-lined stainless steel vessel under autogenous pressure at 165 ℃ for five days. After cooling to room temperature, Red block crystals of complex **1** were collected by filtration and washed with distilled water in 75% yield (based on Mn). Anal. Calcd.(%) for $C_{44}H_{28}N_8O_5Mn$ (**1**): C, 65.76; H, 3.51; N, 13.94. Found (%): C, 65.74; H, 3.52; N, 13.93. IR (KBr, cm^{-1}): 3 062 (m), 1 689 (m), 1 602 (s), 1 543 (s), 1 404 (s), 1 326 (m), 1 247 (m), 1 159 (m), 885 (m), 777 (m), 668 (m), 551 (w), 424 (w).

[Mn_2(4,4′-oba)$_2$(MOPIP)$_4$]·2H_2O (**2**): Complex **2** was also synthesized by a method similar to that described for the synthesis of **1** except that MOPIP (0.163 g, 0.5 mmol) was used instead of Medpq. Red film crystals of complex **2** were collected by filtration

and washed with distilled water in 65% yield (based on Mn). Anal. Calcd.(%) for $C_{108}H_{72}N_{16}O_{14}Mn_2$(**2**): C, 67.29; H, 3.76; N, 11.63. Found (%): C, 67.27; H, 3.75; N, 11.65. IR (KBr, cm^{-1}): 3 400 (m), 3 066 (m), 1 693 (m), 1 609 (s), 1 551 (s), 1 407 (s), 1 350 (m), 1 253 (m), 1 160 (m), 826 (w), 720 (s), 672 (m), 559 (w), 444 (w).

[Cd(ox)(MOPIP)$_2$]·2H$_2$O (**3**): Complex **3** was also synthesized by using a method similar to that described for the synthesis of **2** except that H_2ox (0.063 g, 0.5 mmol) was used instead of 4,4′-H_2oba. Yellow block crystals of complex **3** were collected by filtration and washed with distilled water in 58% yield (based on Cd). Anal. Calcd.(%) for $C_{42}H_{34}N_8O_9Cd$ (3): C, 55.61; H, 3.78; N, 12.35. Found (%): C, 55.60; H, 3.76; N, 12.36. IR (KBr, cm^{-1}): 3 448 (m), 3 072 (m), 1 613 (s), 1 519 (m), 1 481 (s), 1 350 (m), 1 256 (m), 1 171 (m), 804 (w), 738 (s), 701 (w), 512 (w), 418 (w).

1.4 X-ray crystallography

X-ray diffraction data for compounds **1**~**3** were collected on a Rigaku Saturn 724 CCD diffractometer, equipped with a graphite monochromatic Mo $K\alpha$ radiation for compounds **1** and **3**, and Cu $K\alpha$ radiation for compound **2** (λ=0.071 073 nm), by using a φ-ω scan mode at 293(2) K. The structures were solved by direct methods implemented in SHELXS-97[26] and refined by a full-matrix least-squares procedure based on F^2 using SHELXL-97[27]. All non-hydrogen atoms were refined anisotropically, whereas the hydrogen atoms were placed at calculated positions and treated using appropriate riding models. The H-atoms of water molecules in complex **3** could not been positioned reliably. The detailed crystallographic data and structure refinement parameters for the three complexes are listed in Table 1. Selected bond lengths and angles are listed in Table S1 (Supporting Information). The crystal structure representation of complexes **1**~**3** were made by the software DIAMOND[28].

CCDC: 1021348, **1**; 1021349, **2**; 1021347, **3**.

Table 1　Crystal data and structure refinements for compounds 1~3

Complex	**1**	**2**	**3**
Empirical formula	$C_{44}H_{28}N_8O_5Mn$	$C_{108}H_{76}N_{16}O_{16}Mn_2$	$C_{42}H_{32}N_8O_9Cd$
Formula weight	803.68	1 962.72	905.17
Crystal system	Monoclinic	Triclinic	Monoclinic
Space group	$P2_1/c$	$P\bar{1}$	$C2/c$
a / nm	1.169 7(2)	1.629 90(1)	1.809 4(4)
b / nm	2.537 8(5)	1.696 19(1)	1.102 6(2)
c / nm	1.498 4(5)	1.850 09(1)	1.972 9(4)
α / (°)	90	65.365(7)	90
β / (°)	125. 37(2)	75.593(8)	115.29(3)
γ / (°)	90	78.021(9)	90
V / nm^3	3.627 0(15)	4.471 6(5)	3.558 8(142)
Z	4	2	4
D_c / ($g\cdot cm^{-3}$)	1.472	1.458	1.689
F(000)	1 652	2 026	1 840
R_{int}	0.030 8	0.041 9	0.045 0
Reflections collected	16 725	40 770	8 181
Independent reflections	7 153	17 642	3 409
Observed reflections	5 959	12 535	2 997
GOF on F^2	1.068	1.008	1.066
R_1[a] [$I>2\sigma(I)$]	0.066 5	0.061 0	0.048 7
wR_2[b] [$I>2\sigma(I)$]	0.173 6	0.131 4	0.091 7

[a]$R_1=\sum||F_o|-|F_c||/\sum|F_o|$; [b]$wR_2=\{\sum w(|F_o|^2-|F_c|^2)^2/\sum[w(|F_o|^2)]^2\}^{1/2}$

2 Results and discussion

2.1 Structural analysis of complexes 1-3

2.1.1 Crystal structure of {[Mn(4,4′-oba)(Medpq)]Medpq}$_n$ (**1**)

The X-ray single-crystal structure determination of complex **1** suggests that it exhibits a double chain structure. The asymmetric unit of complex **1** consists of one Mn(Ⅱ) ion, one Medpq ligand, one 4,4′-oba anion and one uncoordinated Medpq ligand. As shown in Fig.1a, each Mn(Ⅱ) center is surrounded in a distorted octahedral geometry consisting of two nitrogen atoms from the Medpq chelating ligand, four oxygen atoms from three carboxylic groups of three separated 4,4′-oba anions. The distances Mn-N and Mn-O fall in the reported range[15].

The 4,4′-oba ligand exhibits differences in their connectivity with Mn(Ⅱ) ions. Out of two carboxylates present in one 4,4′-oxybis(benzoic acid), one carboxylate group is coordinated in a bridging bidentate mode, whereas the other is coordinated in a chelating bidentate mode, as depicted in Scheme 1 (coordination mode (a)). The neighboring Mn(Ⅱ) centers are separated at a distance of 0.450 95 nm and are bridged by two carboxylates to form a dinuclear [Mn_2N_4(4,4′-oba)$_2$] unit. The dinuclear unit may be viewed as the basic

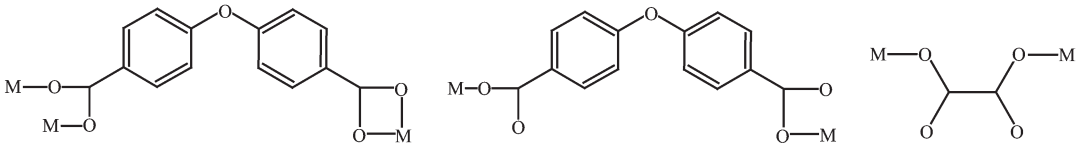

Scheme 1 Coordination modes of carboxylic groups in complexes **1**~**3**

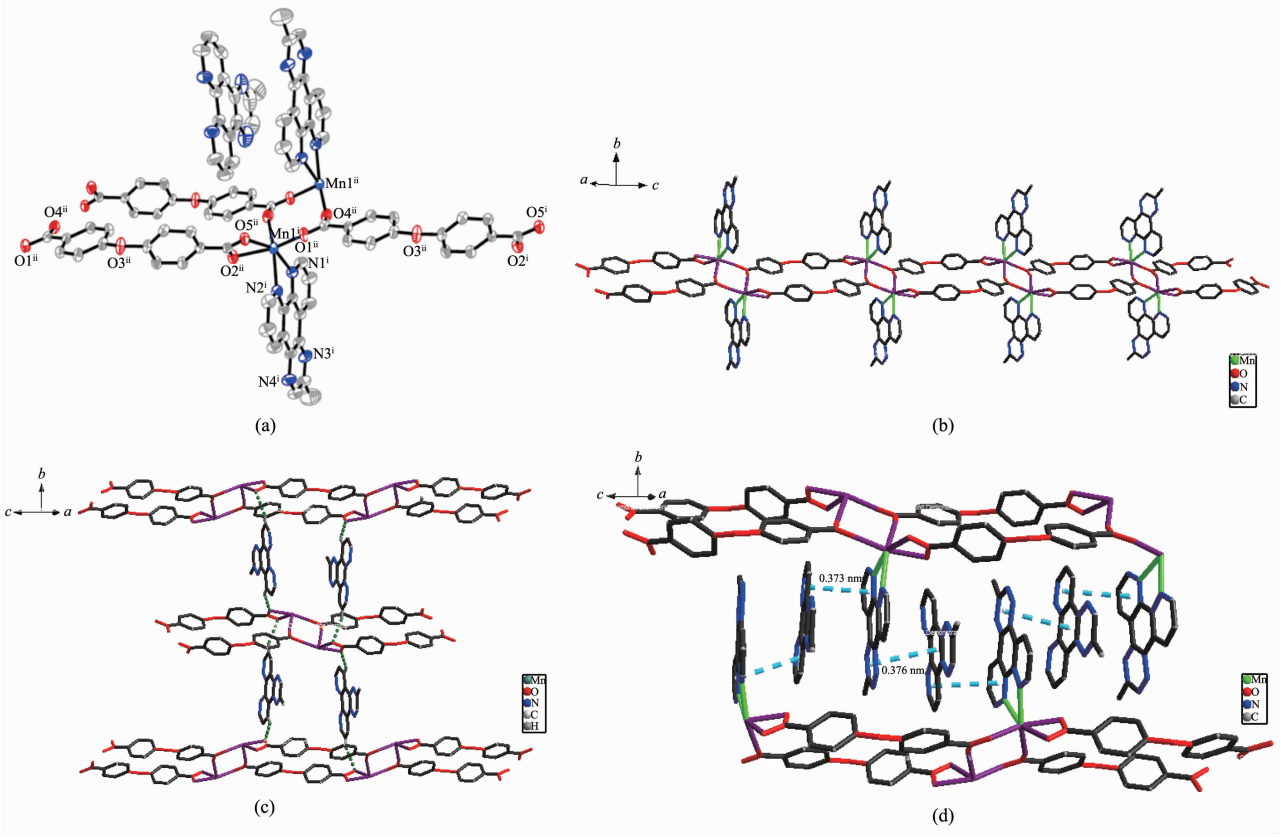

Fig.1 (a) View of the coordination environment of Mn(Ⅱ) in complex **1** (Symmetry code: ^{i}: x, y, $z-1$; Thermal ellipsoids are drawn at the 30% probability level; Hydrogen atoms have been omitted for clarity); (b) View of the linkage of the dinuclear core to the double chain of complex **1**; (c) Supramolecular architecture constructed by hydrogen bonding interactions; (d) Layer structure constructed by $\pi\cdots\pi$ stacking interactions

unit, which is connected to the double chain by carboxylic groups of 4,4′-oba ligands (Fig.1b). The Medpq ligands are attached to both sides of the double chain. It should be pointed out that the coordination mode of 4,4′-oba anion was very different from the related complex $[Pb_2(oba)(dpdp)_2](NO_3)_2 \cdot 2(dpdp) \cdot 2H_2O$ (dpdp=dipyrido [3,2-*a*:2,3-*c*]-phenazine) reported by Yang et al.[12], in which two carboxylate groups of 4,4′-oba anion only adopt the chelating bidentate mode to form a dinuclear unit.

Additionally, the hydrogen bonding interactions between uncoordinated Medpq ligand and 4,4′-oba have been observed in **1**; interchain C–H ⋯ O hydrogen bonds (Table S2, Supporting Information) assemble the neighboring chain along the b axis into a layer structure (Fig.1c). Significant π interactions are also implicated for the reinforcement and overall stability of the crystal lattice. Complex **1** exhibits face-to-face $\pi \cdots \pi$ interactions between Medpq rings at a centroid-to-centroid distance of 0.373 and 0.376 nm, as depicted in Fig.1d.

2.1.2 Crystal structure of $[Mn_2(4,4'\text{-oba})_2(MOPIP)_4] \cdot 2H_2O$ (**2**)

To investigate the influence of the 5,6-substituted 1,10-phen derivative on the frameworks formation of complex, we selected the MOPIP as N-donor ligand to react with manganese salt in the presence of the same 4,4′-oba anions and obtained one new complex $[Mn_2(4,4'\text{-oba})_2(MOPIP)_4]$. As shown in Fig.2a, each Mn(Ⅱ) center is coordinated by two symmetrically bridging carboxylic groups of 4,4′-oba ligand and two chelating MOPIP ligands. Thus, each Mn(Ⅱ) center is hexa-coordinated in a distorted octahedral geometry consisting of four nitrogen atoms from the MOPIP rings and two oxygen atoms from two carboxylic groups of two different 4,4′-oba ligands.

The carboxylate group present in the 4,4′-oxybis (benzoic acid) molecule acts in the bridging monodentate mode, as shown in Scheme 1 (coordination mode (b)), and links a pair of neighboring Mn(Ⅱ) ions to form a dinuclear $[Mn_2N_8(4,4'\text{-oba})]$ unit with a Mn-Mn distance of 1.198 15 nm. The independent dinuclear units are packing through face-to-face $\pi \cdots \pi$ interactions between the imidazole and terminal benzene rings with a centroid-to-centroid distance of 0.398 nm, and edge-to-face $\pi \cdots \pi$ interactions between terminal benzene units with a centroid-to-face distance of 0.387 nm, which result in the formation of a layer structure as presented in Fig.2b. Complex **2** also exhibits strong N–H⋯O hydrogen bonds (Table S2, Supporting Information) between MOPIP rings and 4,4′-oba molecules (Fig.2c). Such interactions lead the layer structure reinforcement and overall stability.

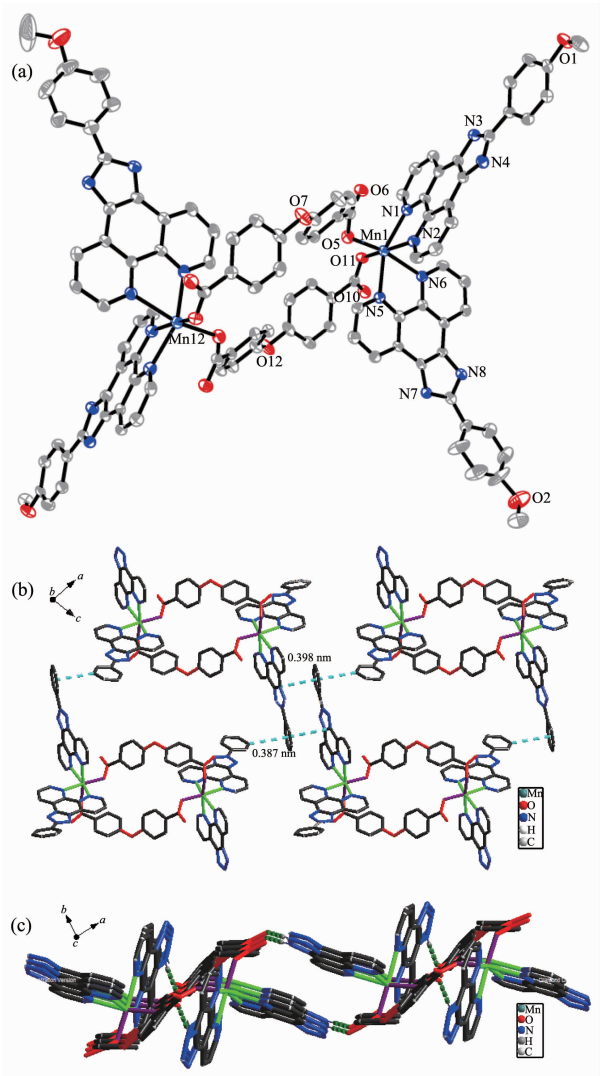

Fig.2 (a) View of the coordination environment of Mn(Ⅱ) in complex **2** (Thermal ellipsoids are drawn at the 30% probability level; Hydrogen atoms have been omitted for clarity); (b) Layer structure constructed by $\pi \cdots \pi$ stacking interactions; (c) Supramolecular architecture constructed by hydrogen bonding interactions

2.1.3 Crystal structure of $[Cd(ox)(MOPIP)_2]\cdot 2H_2O$ (**3**)

To evaluate the effect of the flexibility (the spacer length of carboxyl groups and the structural rigidity of the spacer) of dicarboxylate ligands on the framework formation of complex, we selected oxalic acid to react with cadmium salt. The complex **3** consisting of a mononuclear structure with a smaller pitch than **2** was obtained. Each Cd (Ⅱ) center exhibits octahedral geometry involving two oxygen atoms of two symmetrically monodentate carboxylate groups, along with four nitrogen atoms from two MOPIP molecules and two uncoordinated water molecules, as shown in Fig.3a.

In complex **3**, two carboxylic groups of ox anion all adopting monodentate coordination modes, as depicted in Scheme 1 (coordination mode (c)), and link Cd(Ⅱ) ions to the mononuclear clusters (Fig.3b). The packing of the mononuclear clusters is dominated by face-to-face $\pi\cdots\pi$ interactions between the imidazole and terminal benzene rings with a centroid-to-centroid distance of 0.380 nm, extending the clusters along the a axis into a chain structure (Fig.3b). The most interesting feature of the structure is that it contains strong O–W ⋯ O hydrogen bonding between uncoordinated water molecules and oxygen atoms of carboxylate groups, and C–H⋯O, N–H⋯O hydrogen bonding (Table S2, Supporting Information) between MOPIP molecules and oxygen atoms of carboxylate groups as presented in Fig.3c. Such hydrogen bonding networks cross-link each other and lead to the formation of layer structure.

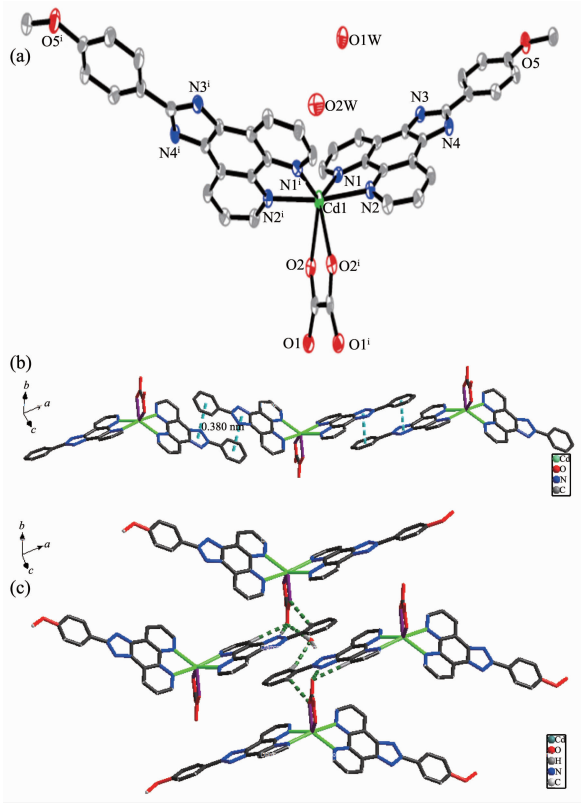

Fig.3 (a) View of the coordination environment of Cd(Ⅱ) in complex **3** (Symmetry code: i: $-x-1, y, -z-1/2$; Thermal ellipsoids are drawn at the 30% probability level; Hydrogen atoms have been omitted for clarity); (b) Chain structure constructed by $\pi\cdots\pi$ stacking interactions; (c) Layer structure constructed by hydrogen bonding interactions

2.2 Effect of N-donor ligands and organic carboxylate anions on the structures of the complexes

As important phen derivatives, the 5,6-substituted 1,10-phen ligands of Medpq and MOPIP both contain an extended π-system, an pyrazine (or imidazole) ring and additional coordination sites, capable of acting as hydrogen bond acceptors/donors or of forming coordination interactions to some metal ions[29]. However, Medpq and MOPIP possess different steric hindrance. The Medpq is a smaller rigid ligand and the 4,4′-oba anion exhibits difference modes, which result in a double chain in **1**. The MOPIP ligand has a comparatively large steric hindrance, which may influence the coordination modes of the carboxylate anions. And the 4,4′-oba anion adopts the bridging monodentate mode, result in a dinuclear structure in **2**. To the aromatic $\pi\cdots\pi$ stacking and hydrogen bonding interactions, the differences of the two ligands are the imidazole ring and additional benzene ring, which may allow the MOPIP ligand to have more chance to assemble higher dimensional complexes in the presence of the bigger N-donor ligand. Complex **1** shows the hydrogen bonding interactions originating from H atom of the Medpq ring and the O atom of carboxylate anion. It is different from MOPIP; the imidazole ring in the MOPIP ligand is a good hydrogen bonding donor. On the other hand, it is noteworthy that the $\pi\cdots\pi$ stacking interactions are found between the imidazole

and terminal benzene rings, and terminal benzene rings in complexes **2**, and play the most important roles in the assembly of supramolecular structures. So, the MOPIP ligands have more important function in the formation of the supramolecular framework.

According to previous reports, the role of organic carboxylate anions can be illustrated in terms of their differences in flexibility. The 4,4′-oxybis(benzoic acid) and oxalic acid were utilized to construct the frameworks of complexes **2** and **3**. In complex **2**, the flexible bridging ligand 4,4′-oba link metal ions to form a dinuclear structure; whereas, for **3**, two carboxylate groups of ox anion adopting monodentate modes links Cd(Ⅱ) ions to the mononuclear clusters. Thus, the presence of ether group (R-O-R) led more bending as well as larger separation of two metal centers, as compared to the mononuclear structure in complex **3**.

2.3 FT-IR analysis

The FT-IR spectra of the compounds **1**~**3** demonstrate strong characteristic absorptions for the carboxylic groups of the 4,4′-oba and ox ligands in the asymmetric and symmetric vibration regions. The asymmetric stretching vibration $\nu_{as}(COO^-)$ appears in the range of 1 613~1 602 cm^{-1}, and 1 350~1 326 cm^{-1} for the symmetric stretching vibration $\nu_s(COO^-)$. The difference ($\Delta\nu$ =276 ~259 cm^{-1} for **1**~**3**) between $\nu_s(COO^-)$ and $\nu_{as}(COO^-)$ is much more than that of an ionic carboxylate unit, which indicates that carboxylic groups are monodentate coordinated with metal ions, which is in agreement with the crystal structure[30]. The band at 559~512 cm^{-1} for compounds **1**~**3** also proves the coordination of metal ions and nitrogen atoms. The band at 444~418 cm^{-1} for **1**~**3** indicates that the metal ions are coordinated with oxygen atoms[31]. The broad bands at around 3 448~3 400 cm^{-1} are attributed to the vibrations of water molecules.

2.4 Thermal properties

Thermal stability of the compounds **1**~**3** were performed by using thermogravimetric (TG) analyzer (Fig.4). The compound 1 shows a three-step weight loss. The first weight loss of 29.97% (Calcd. 30.64%) occurs from 202 to 356 ℃, which corresponds to the loss of one equivalent of free Medpq ligands. The second weight loss of 32.01% (Calcd. 31.88%) between 356 and 550 ℃ is ascribed to the loss of 4,4′-oba ligand per formula unit. The last weight loss of 29.05% (Calcd. 30.64%) in the range of 550 to 1128 ℃ is corresponded to the loss of one Medpq ligand coordinated with Mn(Ⅱ) ion. After the decomposition, the final product may be MnO. For complex **2**, the framework begins to collapse at 224 ℃, which is assigned to the release of 4,4′-oba ligands (Obsd. 26.59%, Calcd. 26.58%), and the departure of MOPIP ligands occur from 541 to 1 121 ℃ (Obsd. 66.13%, Calcd. 67.72%). The weight losses are in agreement with the theoretical volume of the crystal structure, with MnO forms as the final remnant. For **3**, the framework begins to collapse at 100 ℃, which is assigned to the release of free H_2O molecules (Obsd. 5.14 %, Calcd. 5.96%), the departure of ox ligands occur from 251 to 451 ℃ (Obsd. 10.94%, Calcd. 9.70%), and the decomposition of MOPIP ligands occur in the range of 452 to 1 120 ℃ (Obsd. 69.89%, Calcd. 71.95%). The observed total weight loss of 85.97 % is in accordance with the expected value of 85.84%, with CdO forms as the final remnant.

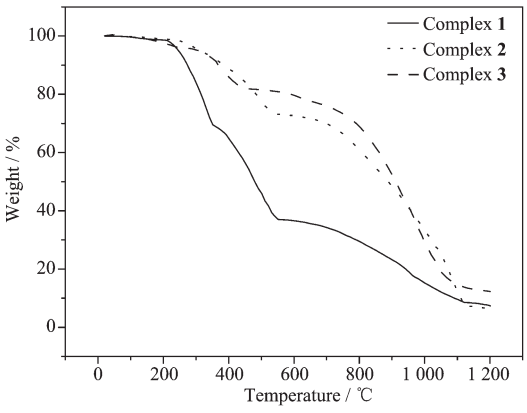

Fig.4 Thermal analyses spectra of complexes **1**~**3**

2.5 Powder X-ray diffraction analyses

To confirm the phase purity of the bulk materials, powder X-ray diffraction (PXRD) experiments were carried out for complexes **2**~**3**, as shown in Fig.5. The experimental PXRD patterns correspond well with the computer-simulated from the single crystal data, indicating the high purity of the synthesized samples.

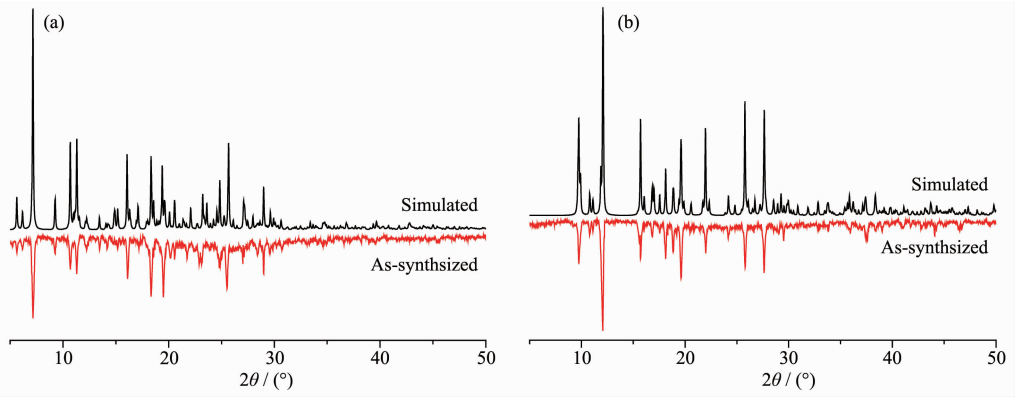

Fig.5 Comparison of PXRD patterns of the simulated pattern from the single-crystal structure determination and the as-synthesized products of complexes **2** (a) and **3** (b)

The differences in reflection intensities between the simulated and the experimental pattern are due to the variation in preferred orientation of the powder samples[32].

2.6 Fluorescent properties

The solid-state fluorescence spectra of **2**~**3** were recorded at room temperature. The free MOPIP ligand also display emission with one main emission peaks at 469 nm upon excitation at 361 nm (Fig.S1), which probably be assigned to the $\pi \rightarrow \pi^*$ transitions. The emission peaks of **2** at 467 nm (λ_{ex}=361 nm) are mainly from the MOPIP ligand. The complex **3** exhibits a little red shift with the bands at 485 nm (λ_{ex}=306 nm). The red shift emission peak probably is related to the intraligand fluorescent emission, and similar red shifts have been observed before[33-34]. The difference of their topological structures results in that the emission bands of **2**~**3** is diverse. The result indicates that the fluorescence behavior is closely associated with the metal ions and the ligands coordinated around them.

2.7 Natural Bond Orbital (NBO) Analysis

The selected natural electron configuration, Wiberg bond indexes, and NBO bond order (a.u.) for compound **1** and **3** are shown in Table 2. It can be concluded that the Mn(Ⅱ) ion coordinating to O and N atoms is mainly on 4*s* and 3*d* orbits and Cd(Ⅱ) is mainly on 5*s* and 4*d* orbits (the electron number of other orbits is so small that can be omitted)[35]; O atoms and N atoms bonding with Mn(Ⅱ) and Cd(Ⅱ)ion

Table 2 Natural atomic charges, natural valence electron configurations, wiberg bond indexes and NBO bond orders (a.u.) for compounds 1 and 3

Atom	Net charge / e	Valence electron configuration	Bond	Wiberg bond index	NBO bond order
Mn	1.286 19	[core]4*s*(0.20)3*d*(5.49)4*p*(0.01)4*d*(0.01)			
O4^{ii}	−0.749 20	[core]2*s*(1.72)2*p*(5.01)3*p*(0.01)3*d*(0.01)	Mn-O4^{ii}	0.191 0	0.144 6
O5^{ii}	−0.709 15	[core]2*s*(1.72)2*p*(4.96)3*s*(0.01)3*d*(0.02)	Mn-O5^{ii}	0.205 8	0.119 7
O1^{i}	−0.814 02	[core]2*s*(1.70)2*p*(5.08)3*p*(0.03)	Mn-O1i	0.290 1	0.199 4
O2^{ii}	−0.797 48	[core]2*s*(1.67)2*p*(5.11)3*p*(0.01)	Mn-O2^{ii}	0.242 5	0.210 1
N1^{i}	−0.477 76	[core]2*s*(1.35)2*p*(4.09)3*p*(0.02)3*d*(0.01)4*p*(0.01)	Mn-N1^{i}	0.235 0	0.175 2
N2^{i}	−0.455 80	[core]2*s*(1.34)2*p*(4.09)3*p*(0.02)4*p*(0.01)	Mn-N2^{i}	0.210 2	0.162 3
Cd	1.734 62	[core]5*s*(0.26)4d(9.99)5*p*(0.01)6*p*(0.01)			
N1	−0.525 80	[core]2*s*(1.35)2*p*(4.14)3*s*(0.01)3*p*(0.02)3*d*(0.01)4*p*(0.01)	Cd-N1	0.066 2	0.080 8
N2	−0.535 39	[core]2*s*(1.35)2*p*(4.14)3*s*(0.01)3*p*(0.02)4*p*(0.01)	Cd-N2	0.066 4	0.083 3
N1^{i}	−0.515 59	[core]2*s*(1.36)2*p*(4.13)3*p*(0.01)4*p*(0.01)	Cd-N1^{i}	0.062 9	0.077 4
N2^{i}	−0.521 09	[core]2*s*(1.36)2*p*(4.13)3*p*(0.01)4*p*(0.01)	Cd-O2^{i}	0.062 7	0.078 4
O2	−0.890 21	[core]2*s*(1.71)2*p*(5.15)3*s*(0.01)3*p*(0.01)3*d*(0.01)	Cd-O2	0.071 6	0.081 4
O2^{i}	−0.874 66	[core]2*s*(1.71)2*p*(5.15)3*p*(0.01)	Cd-O2^{i}	0.072 6	0.065 6

are all on 2*s* and 2*p* orbits (the electron number of 3*p* orbit is so small that can be omitted). Therefore, the Mn(Ⅱ) (or Cd(Ⅱ)) ion obtains some electrons from MOPIP and 4,4′-oba (or ox) ligand. The differences of their bond lengths make the NBO bond orders different[36], which is good agreement with the X-ray crystal structural data of compounds **1** and **3**.

Fig.S2 shows the lowest unoccupied (LUMO) and the highest occupied molecular orbitals (HOMO) of the complexes **1** and **3**. For complex **1**, the LUMO orbitals is mainly composed of π orbits of 4,4′-oba ligand. For **3**, the LUMO orbitals are concentrated mainly in the center of the molecules and composed of π orbits of MOPIP. On the other hand, For complex **1**, The highest occupied molecular orbitals (HOMO) consists of π orbits mainly from MOPIP and 4,4′-oba ligand. For **3**, HOMO levels show greater contributions from π orbits of ox anion, some contributions from π orbits of MOPIP, and smaller contributions from d orbit in Cd (Ⅱ) ion in compound **3**. So, ligands to ligands charge transition may be inferred from some contours of molecular orbitals of complex **1**. In the same way, ligands to ligands and ligand-metal charge transition may be inferred from some contours of molecular orbitals of complex **3**.

3 Conclusions

Three metal-organic coordination complexes of divalent metal ions with 5,6-substituted 1,10-phen derivatives, 4,4′ -oba and ox ligand have been successfully synthesized by hydrothermal reaction. The structures of these compounds are distinct from one another. The results imply that the size of the N-heterocyclic chelating ligands and the flexibility of carboxylate have a significant influence on the structure of the compounds. The combination of 5,6-substituted 1,10-phen derivatives and carboxylate ligands with metal centers might form coordination polymers with interesting structures and topologies.

Acknowledgement: This work is supported by the Programs of Senior Talent Foundation of Jiangsu University (No. 14JDG053) and Jiangsu Postdoctoral Science Foundation (No. 1401176C).

Supporting information is available at http://www.wjhxxb.cn

References:

[1] Ohrstrom L, Larsson K. *Dalton. Trans.*, **2004**,**3**:347-353

[2] Yadav P K, Kumari N, Pachfule P, et al. *Cryst. Growth Des.*, **2012**,**12**:5311-5319

[3] Sun C Y, Gao S, Jin L P. *Eur. J. Inorg. Chem.*, **2006**,**12**: 2411-2421

[4] Rosi N L, Eckert J, Eddaoudi M, et al. *Science*, **2003**,**300**: 1127 -1130

[5] Wang X L, Qin C, Wang E B. *Cryst. Growth Des.*, **2006**,**6**: 439-443

[6] Pasan J, Sanchiz J, Lloret F, et al. *Cryst. Eng. Comm.*, **2007**, **9**:478-487

[7] Ma L F, Wang Y Y, Wang L Y, et al. *Eur. J. Inorg. Chem.*, **2008**,**5**:693-703

[8] Zhang W H, Wang Y Y, Lermontova E K, et al. *Cryst. Growth Des.*, **2010**,**10**:76-84

[9] Wang C J, Yue K F, Tu Z X, et al. *Cryst. Growth Des.*, **2011**, **11**:2897-2904

[10]Furukawa H, Kim J, Ockwig N W, et al. *J. Am. Chem. Soc.*, **2008**,**130**:11650-11661

[11]Li M X, Miao Z X, Shao M, et al. *Inorg. Chem.*, **2008**,**47**: 4481-4489

[12]Yang J, Ma J F, Liu Y Y, et al. *Inorg. Chem.*, **2007**,**46**:6542 -6555

[13]Wang X L, Chen Y Q, Gao Q, et al. *Cryst. Growth Des.*, **2010**,**10**:2174-2184

[14]Wang L, Ni L. *J. Coord. Chem.*, **2012**,**65**:1475-1483

[15]Wang L, Ni L, Yao J. *Polyhedron*, **2013**,**59**:115-123

[16]HUANG Yan-Ju(黄燕菊), NI Liang(倪良), DU Gang(杜刚), et al. *Chinese J. Inorg. Chem.*(无机化学学报), **2010**,**26**(7): 1269-1273

[17]Shi Z Q, Li Y Z, Guo Z J, et al. *Cryst. Growth Des.*, **2013**, **13**:3078-3086

[18]Mahata P, Draznieks C M, Roy P, et al. *Cryst. Growth Des.*, **2013**,**13**:155-168

[19]Xu G H, He X Y, Lü J Y, et al. *Cryst. Growth Des.*, **2012**, **12**:3619-3630

[20]Mahata P, Natarajan S, Panissod P, et al. *J. Am. Chem. Soc.*, **2009**,**131**:10140-10150

[21]Manjunatha M N, Dikundwar A G, Nagasundara K R. *Polyhedron*, **2011**,**30**:1299-1304

[22]Tatjana S R, Manja Z, Tamara T, et al. *Eur. J. Med. Chem.*,

2011,**46**:3734-3747

[23]Zampakou M, Rizeq N, Tangoulis V, et al. *Inorg. Chem.*, **2014**,**53**:2040-2052

[24]Wang L, Ni L, Zhao J, et al. *Z. Anorg. Allg. Chem.*, **2012**, **38**:224-230

[25]Frisch M J, Trucks G W, Schlegel H B. *Gaussian* 03 *Revision B*. 03, Gaussian, Inc., Pittsburgh PA, **2003**.

[26]Sheldrick G M. *SHELXS*-97, *Program for Solution of Crystal Structures*, University of Göttingen, Germany, **1997**.

[27]Sheldrick G M. *SHELXL*-97, *Program for Refinement of Crystal Structures*, University of Göttingen, Germany, **1997**.

[28]Pennington W T. *J. Appl. Cryst.*, **1999**,**32**:1028-1029

[29]Wang X L, Chen Y Q, Gao Q, et al. *Cryst. Growth Des.*, **2010**,**10**:2174-2184

[30]Shi X, Zhu G S, Wang X H, et al. *Cryst. Growth Des.*, **2005**,**5**:341-346

[31]Nakamoto K. *Infrared and Raman Spectra of Inorganic and Coordination Compounds*. 4*th Ed*. New York: Wiley Interscience, **1986**.

[32]Shan W W, Ma S S, Wang H L, et al. *J. Inorg. Organomet. Polym.*, **2014**,**24**:468-475

[33]Wang C C, Wang Z H, Gu F B, et al. *J. Mol. Struct.*, **2011**, **1004**:39-44

[34]Shi X, Zhu G, Fang Q, et al. *Eur. J. Inorg. Chem.*, **2004**,**1**: 185-191

[35]Peng X, Cui G H, Li D J, et al. *J. Mol. Struct.*, **2010**,**967**: 54-60

[36]LI Zhang-Peng(李章鹏), XING Yong-Heng(邢永恒), ZHANG Yuan-Hong(张元红). *Acta Phys.-Chim. Sin.*(物理化学学报), **2009**,**25**(4):741-746